ISSN: 0973-3469, Vol.17, (Special Issue) 2020, Pg. 27-40

Material Science Research India

www.materialsciencejournal.org

Molecular Structure, Electronic, Chemical and Spectroscopic (UV-Visible and IR) Studies of 5-(4-Chlorophenyl)-3-(3,4-dimethoxyphenyl)-1-phenyl-4,5-dihydro-1*H*-pyrazole: Combined DFT and Experimental Exploration

SANDIP S. PATHADE[1], VISHNU A. ADOLE[2], BAPU S. JAGDALE[2] and THANSING B. PAWAR[3]*

[1]Department of Chemistry, Maharaja Sayajirao Gaikwad Arts, Science and Commerce College Malegaon, (Affiliated to SP Pune University) Nashik-423 105, India.

[2]Department of Chemistry, Arts, Science and Commerce College, Manmad, (Affiliated to SP Pune University) Nashik-423 104, India.

[3]Department of Chemistry, Loknete Vyankatrao Hiray Arts, Science and Commerce College Panchavati, (Affiliated to SP Pune University) Nashik-422 003, India.

Abstract

The current examination deals with a detailed investigation on the computational study of 5-(4-chlorophenyl)-3-(3,4-dimethoxyphenyl)-1-phenyl-4,5-dihydro-1H-pyrazole (CPMPP) by using density functional theory (DFT). CPMPP is synthesized and characterized by UV-Visible, FT-IR, 1H NMR, and ^{13}C NMR spectroscopic methods. The molecular structure, optimized geometrical parameters, and vibrational assignments have been established employing the DFT method, the B3LYP method, and the 6-311++G (d,p) basis set. Frontier molecular orbital (FMO) analysis and various global reactivity parameters are also discussed for the better comprehension of the chemical reactivity. Theoretical and Experimental; UV-Visible analysis is compared and a good deal of agreement is found. Experimental vibrational frequencies were compared with the theoretical IR spectrum to mark the correct vibrational assignments. Molecular electrostatic surface potential (MESP) and Mulliken atomic charges are computed at the same level of theory to locate the charge density. Absorption energies, excitation energy, oscillator strength, and transitions have been computed at TD-B3LYP/6-311++G (d,p) level of theory for B3LYP/6-311++G (d,p) optimized geometry.

Article History

Received: 21 June 2020
Accepted: 25 July 2020

Keywords:

DFT;
Gaussian;
Molecular Structure;
Vibrational Assignments;
5-(4-Chlorophenyl)-3-(3,4-dimethoxyphenyl)-1-phenyl-4,5-dihydro-1H-pyrazole.

CONTACT Thansing B. Pawar Pawartbpawar03@gmail.com Department of Chemistry, Loknete Vyankatrao Hiray Arts, Science and Commerce College Panchavati, (Affiliated to SP Pune University) Nashik-422 003, India.

Doi: http://dx.doi.org/10.13005/msri.17.special-issue1.05

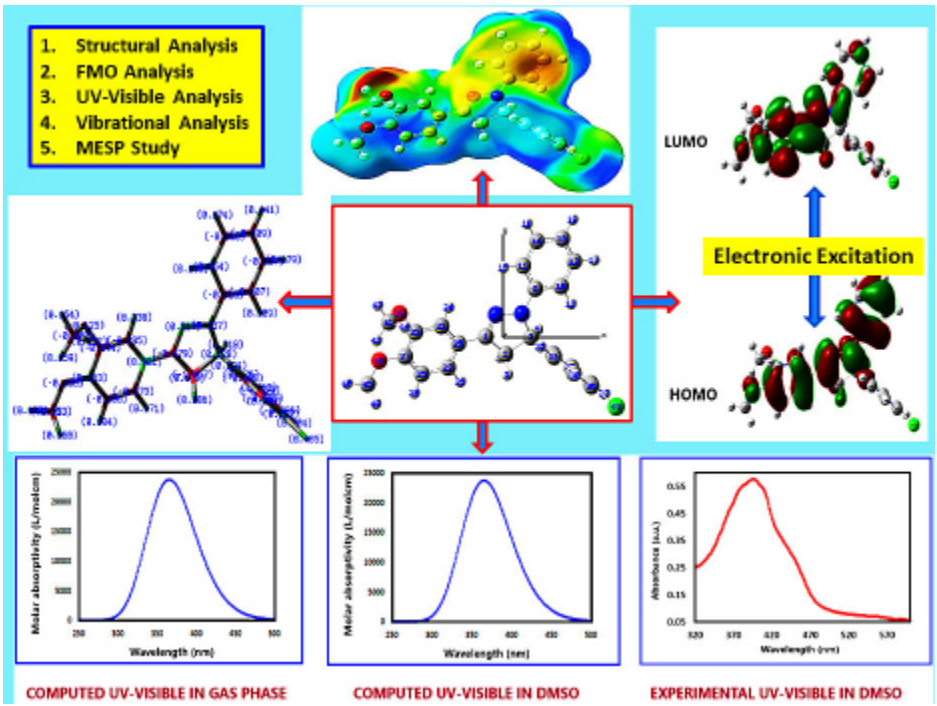

Graphical abstract

Introduction

Pyrazoles are five-membered heterocycles that establish a class of heterocyclic compounds especially valuable in organic synthesis. Pyrazoline is one of the imperative synthons in therapeutic science and has played a crucial role in the development of heterocyclic compounds. The chalcones are significant intermediates for the synthesis of various heterocyclic compounds including pyrazolines. Pyrazole frameworks have pulled in more consideration because of their fascinating pharmacological properties.[1-3] The wide range of biological properties includes anticancer activity,[4] anti-tubercular,[5] antibacterial,[6] antifungal ,[7] anti-inflammatory,[8] analgesic,[9] anti-viral activity,[10] anti-diabetic,[101] anti-malarial,[12] etc. Few examples of biologically potent drugs containing pyrazole structure are given in Figure 1. Lonazolac is found to show excellent anti-inflammatory activity in disease treatments whereas fezolamine shows anti-depressant and difenamizole shows analgesic activity. The green chemistry has advanced in recent years and explored for the synthesis of variety of organic compounds having potential biological applications.[13-20] The PEG solvents have been used to increase environmental sustainability and energy-efficient reactions.[21-23]

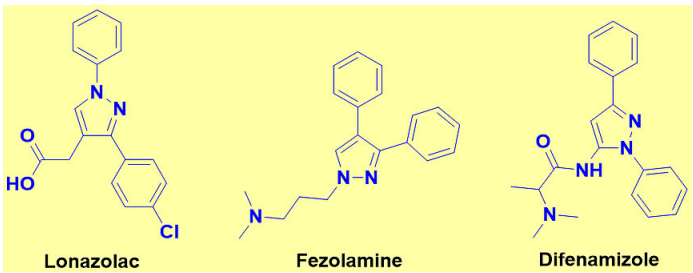

Fig.1: Biologically potent drug containing pyrazole structure

Theoretical chemistry based on DFT can predict various molecular properties. By virtue of DFT, different spectroscopic assessments can be achieved; UV-Visible spectra, IR and Raman frequencies, NMR chemical shifts, and spin-spin coupling constants.[24-32] Also, DFT calculations can anticipate FMO energies, bond lengths, bond angles, dihedral angles, absorption energies, etc.[33-45] The comparison of theoretical calculations with experimental outcomes gives decent information. Critically, the examination of the reaction mechanisms is made simpler because of calculation estimations in view of DFT. Considering all these critical angles and continuation of our enthusiasm for synthesizing heterocyclic compounds, we wish to report synthesis and density functional theory investigation of 5-(4-chlorophenyl)-3-(3,4-dimethoxyphenyl)-1-phenyl-4,5-dihydro-1*H*-pyrazole. In the current investigation various structural, spectroscopic, and quantum chemical facets of title compound have been revealed.

Experimental

Material and Methods

All the chemicals needed for synthesis were obtained from a commercial source (AR grade with purity > 99%) and used without further purification. Melting points of the compounds were determined in an open capillary tube and is uncorrected, IR spectra were recorded on the Shimadzu FT-IR spectrometer using potassium bromide pellets. ^{1}H NMR was determined on Bruker Advance II 500 MHz spectrometer using DMSO as a solvent. The UV-Visible analysis was performed within 200 to 800 nm range in the DMSO solvent. The reactions were monitored by thin-layer chromatography (TLC, Merck) using aluminum sheets coated with silica gel by using n-hexane and ethyl acetate as an eluent.

Synthesis of Chalcone

An equimolar mixture of 3,4-dimethoxy acetophenone (1, 0.01 mol) and 4-chloro benzaldehyde (2, 0.01 mol), and 10 % NaOH (10 mL) in ethanol (15 mL) was stirred together for 14 hours at room temperature. The completion of the reaction was monitored by TLC. Then the reaction mixture was poured into crushed ice and acidified with dilute HCl. The solid obtained was filtered, washed with water, dried, and recrystallized from ethanol to obtain desire chalcone.

Synthesis of CPMPP

The solution of chalcone 3 (20 mmol) and phenylhydrazine (20 mmol), and 10% NaOH in PEG-200 (10 mL) were refluxed for 2 hours at 70-80°C. The completion of the reaction was monitored by TLC. After completion of the reaction, the reaction mixture was poured into crushed ice and precipitate obtained was filtered under vacuum, washed with water, dried, and recrystallized from ethanol to furnish the title compound 4. The overall reaction is given in Scheme 1.

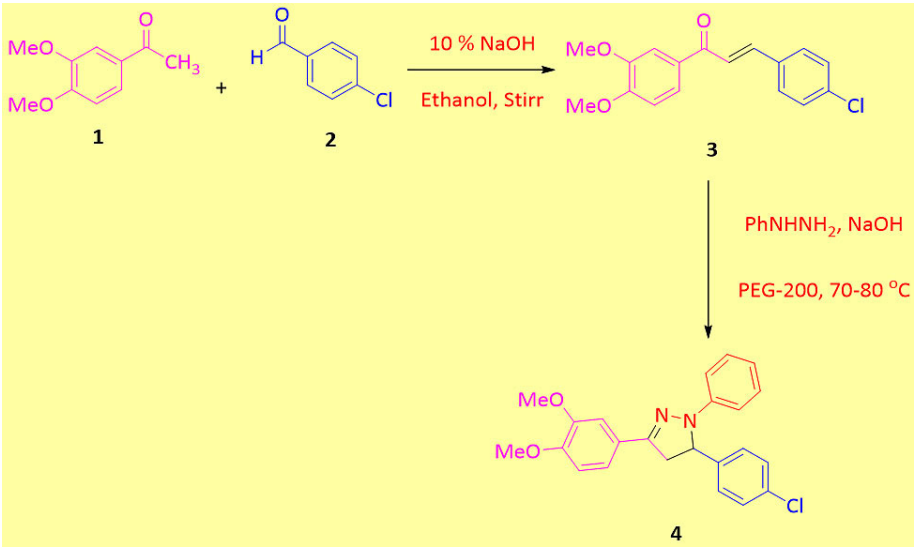

Scheme 1: Synthesis of CPMPP

Physicochemical and Spectral Analysis

Light yellowish solid; Yield: 92 %; m.p. 140-142 °C. FT-IR (KBr, in cm^{-1}): 1596 (C=N str), 2917 (Ar-H str), 1495 (Aro. C=C str), 816 (Ar-Cl str); ^{1}H NMR (500 MHz, $CDCl_3$) δ: 7.49 (d, J = 2.0 Hz, ^{1}H), 7.30 (d, J = 8.5 Hz, 2H), 7.26 (d, J = 6.5 Hz, 2H), 7.20 – 7.16 (m, 2H), 7.02 (m, 3H), 6.84 (d, J = 8.4 Hz, 1H), 6.82 – 6.75 (m, ^{1}H), 5.21 (dd, J = 12.3, 7.2 Hz, 1H), 3.98 (s, 3H), 3.90 (s, 3H), 3.82 (dd, J = 16.9, 12.3 Hz, 1H), 3.08 (dd, J = 16.9, 7.2 Hz, 1H); ^{13}C NMR (126 MHz, $CDCl_3$) δ (ppm): 150.01, 149.17, 146.90, 144.88, 141.20, 133.30, 129.35, 128.98, 127.36, 125.57, 119.19, 119.11, 113.32, 110.62, 108.09, 63.93, 55.97, 43.68.

Computational Details

All the computational calculations are determined in the gas phase by the DFT method using Gaussian-03(W) software. To analyze the theoretical parameters of the titled compound, geometry was optimized by DFT/B3LYP method with a 6-311++G (d,p) basis set [46]. The optimized structure of compounds was used for the calculation of thermodynamic parameters, global chemical reactivity parameters, frontier molecular orbital analysis, and plotting the molecular electrostatic potentials. Absorption energies, excitation energy, oscillator strength, and transitions have been computed at TD-B3LYP/6-311++G (d,p) level of theory for B3LYP/6-311++G (d,p) optimized geometry.

Results and Discussion

Structural Analysis

The optimized molecular structure of the CPMPP is given in Figure 2. Optimized bond lengths and bond angles of CPMPP at B3LYP/6-311++G (d,p) are presented in Table 1. The CPMPP possesses aromatic C=C bond lengths from 1.38 Å to 1.40 Å. The azo group (N7-N8) bond is 1.3708 Å long and the imine (C1=N8) bond is 1.2887 Å in length. The dipole moment of the CPMPP is 4.59 Debye with C1 point group symmetry and -1609.51 a.u. E(B3LYP) energy. The bond angles N8-C1-C20, C1-N8-N7, O40-C45-H47, and C32-C36-Cl49 are 122.6027°, 110.3769°, 111.2483°, and 119.4557° respectively. Other bond length and bond angle data are also in good agreement.

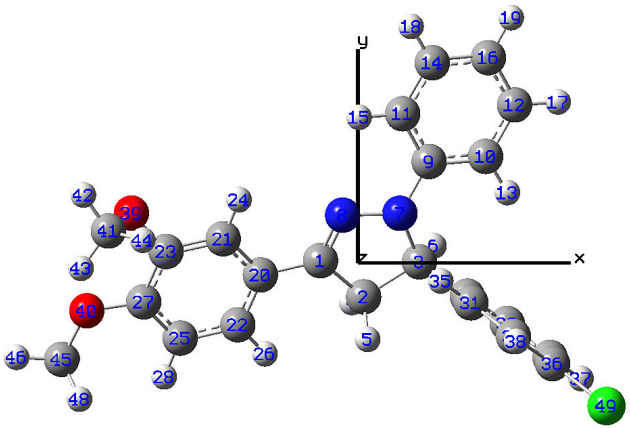

Fig.2: Optimized structure with atomic labeling

Table 1: Optimized bond lengths and bond angles at B3LYP/6-311++G (d,p) level

Bond length (Å)					
C1-C2	1.5164	C12-C16	1.3919	C29-C31	1.3970
C1-N8	1.2887	C12-H17	1.0846	C30-C32	1.3933
C1-C20	1.4612	C14-C16	1.3960	C30-H33	1.0857
C2-C3	1.5542	C14-H18	1.0847	C31-C34	1.3923

C2-H4	1.0930	C16-H19	1.0835	C31-H35	1.0840
C2-H5	1.0931	C20-C21	1.4084	C32-C36	1.3904
C3-H6	1.0962	C20-C22	1.3977	C32-H37	1.0825
C3-N7	1.4793	C21-C23	1.3820	C34-C36	1.3915
C3-C29	1.5202	C21-H24	1.0824	C34-H38	1.0826
N7-N8	1.3708	C22-C25	1.3960	C36-Cl49	1.7595
N7-C9	1.3987	C22-H26	1.0835	O39-C41	1.4325
C9-C10	1.4051	C23-C27	1.4165	O40-C45	1.4223
C9-C11	1.4070	C23-O39	1.3718	C41-H42	1.0895
C10-C12	1.3932	C25-C27	1.3936	C41-H43	1.0920
C10-H13	1.0815	C25-H28	1.0817	C41-H44	1.0957
C11-C14	1.3889	C27-O40	1.3616	C45-H46	1.0886
C11-H15	1.0805	C29-C30	1.3969	C45-H47	1.0950
-	-	-	-	C45-H48	1.0953

Bond angle (°)

C2-C1-N8	112.7333	C10-C12-H17	118.9366	C29-C30-C32	121.1396
C2-C1-C20	124.662	C16-C12-H17	120.0987	C29-C30-H33	119.8456
N8-C1-C20	122.6027	C11-C14-C16	121.1398	C32-C30-H33	119.0141
C1-C2-C3	102.4226	C11-C14-H18	118.9236	C29-C31-C34	120.8973
C1-C2-H4	111.7172	C16-C14-H18	119.9358	C29-C31-H35	119.5406
C1-C2-H5	111.6775	C12-C16-C14	118.7769	C34-C31-H35	119.5533
C3-C2-H4	112.2421	C12-C16-H19	120.5992	C30-C32-C36	118.9867
C3-C2-H5	111.3691	C14-C16-H19	120.6239	C30-C32-H37	120.8066
H4-C2-H5	107.4636	C1-C20-C21	120.9602	C36-C32-H37	120.2055
C2-C3-H6	110.4550	C1-C20-C22	121.0493	C31-C34-C36	119.2429
C2-C3-N7	101.8185	C21-C20-C22	117.9901	C31-C34-H38	120.6664
C2-C3-C29	112.9459	C20-C21-C23	121.5549	C36-C34-H38	120.0897
H6-C3-N7	109.1755	C20-C21-H24	120.0735	C32-C36-C34	121.0291
H6-C3-C29	108.6815	C23-C21-H24	118.3982	C32-C36-Cl49	119.4557
N7-C3-C29	113.5987	C20-C22-C25	121.0966	C34-C36-Cl49	119.5142
C3-N7-N8	112.5815	C20-C22-H26	120.4259	C23-O39-C41	116.2329
C3-N7-C9	124.3649	C25-C22-H26	118.4773	C27-O40-C45	118.5520
N8-N7-C9	119.4649	C21-C23-C27	119.8929	O39-C41-H42	105.9929
C1-N8-N7	110.3769	C21-C23-O39	118.8338	O39-C41-H43	111.3279
N7-C9-C10	120.5477	C27-C23-O39	121.1526	O39-C41-H44	110.4094
N7-C9-C11	120.6239	C22-C25-C27	120.5002	H42-C41-H43	109.6557
C10-C9-C11	118.8234	C22-C25-H28	119.0783	H42-C41-H44	109.3871
C9-C10-C12	120.2049	C27-C25-H28	120.4191	H43-C41-H44	109.9796
C9-C10-H13	120.6123	C23-C27-C25	118.9595	O40-C45-H46	105.7824
C12-C10-H13	119.1746	C23-C27-O40	116.2956	O40-C45-H47	111.2483
C9-C11-C14	120.0902	C25-C27-O40	124.7425	O40-C45-H48	111.4068
C9-C11-H15	119.1303	C3-C29-C30	119.9300	H46-C45-H47	109.3764
C14-C11-H15	120.7787	C3-C29-C31	121.3116	H46-C45-H48	109.3962
C10-C12-C16	120.9644	C30-C29-C31	118.7030	H47-C45-H48	109.5428

Charge Density Distribution Study

Mulliken atomic charges and molecular electrostatic surface potential are studied for the investigation of a charge density distribution study. Mulliken atomic charges are presented in Table 2 and Figure 3. The C2 carbon atom is the most electronegative with a

charge density of -1.06730 whereas C20 carbon atom is the most electropositive carbon atom with charge density of 0.90122. Talking about hydrogen atoms, all hydrogen atoms are electropositive.

Table 2: Mulliken atomic charges

Atom	Charge	Atom	Charge	Atom	Charge
C1	-0.47944	H18	0.17408	H35	0.19404
C2	-1.06730	H19	0.14055	C36	0.25209
C3	0.22775	C20	0.90122	H37	0.20442
H4	0.18280	C21	-0.29498	H38	0.20834
H5	0.18648	C22	-0.27261	O39	-0.12454
H6	0.21757	C23	-0.49427	O40	-0.18626
N7	0.15700	H24	0.23809	C41	-0.30824
N8	0.51666	C25	-0.18568	H42	0.15422
C9	-0.31043	H26	0.17104	H43	0.15928
C10	-0.30652	C27	0.16294	H44	0.13171
C11	0.05379	H28	0.18358	C45	-0.31298
C12	-0.23681	C29	0.42632	H46	0.18028
H13	0.10948	C30	-0.22009	H47	0.15328
C14	-0.16792	C31	-0.49845	H48	0.16010
H15	0.19277	C32	-0.38618	Cl49	0.46538
C16	-0.30929	H33	0.16241	-	-
H17	0.17885	C34	-0.68456	-	-

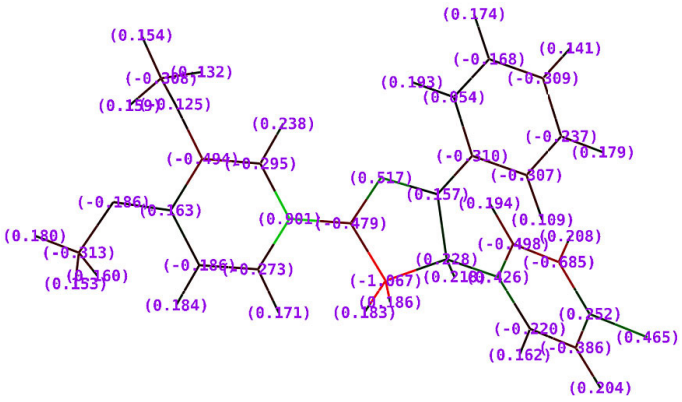

Fig. 3: Mulliken charge distribution

The MESP plot is depicted in Figure 4. The molecular electrostatic potential surface analysis could provide information about the crucial molecular properties like dipole moment, partial charges, and chemical reactivity of the molecules. The presence of various distinct colors indicates the variation in the electron density distribution. The red and yellow colors speak about high electron density, blue and green colors indicate regions with positive and zero electrostatic potentials respectively. The present study of the MESP plot indicates that the phenyl ring attached to a nitrogen atom is highly susceptible to react with the electrophilic reagents and therefore the molecule could undergo electrophilic aromatic substitution reactions at the phenyl ring attached to a nitrogen atom.

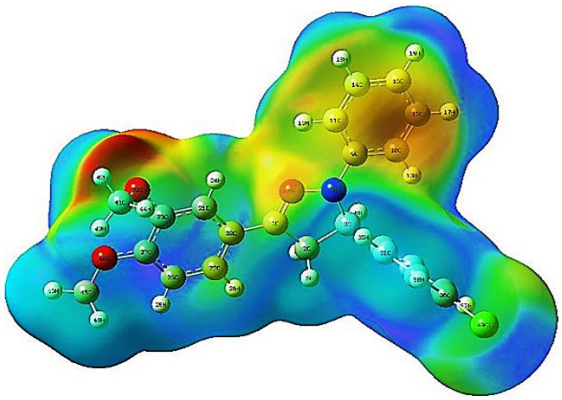

Fig. 4: Mulliken charge distribution

FMO, Electronic and Chemical Reactivity Studies

The pictorial representation of the HOMO-LUMO of the title compound is given in Figure 5. The data of the electronic parameters and the global reactivity descriptors are given in Table 3. The HOMO-LUMO orbitals are called as Frontier Molecular Orbitals (FMO). The energy gap between HOMO-LUMO is a fundamental pointer of kinetic stability. The assessment of the wave function indicates that the electron absorption corresponds to the transition from the HOMO to the LUMO and is mostly portrayed by one electron promotion. The Koopmans' hypothesis has been utilized for the examination of the global reactivity descriptor parameters and because of frontier molecular orbital energies, the different parameters such as ionization potential (I), electron affinity (A), band gap (Eg), electronegativity (χ), absolute hardness (η), global softness (S), global electrophilicity (ω), chemical potential (μ), and maximum no. of electron transferred (ΔNmax) have been built up.

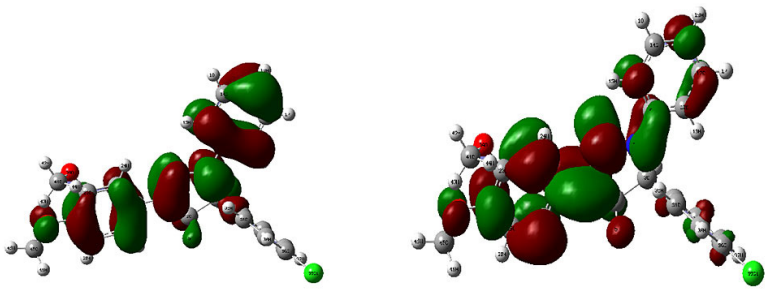

Fig. 5: Frontier molecular orbitals

Table 3: Global chemical reactivity descriptors

Molecular Properties	Value
EHOMO	-5.1838 eV
ELUMO	-1.3954 eV
ΔE (ELUMO-EHOMO)	3.7884 eV
Ionisation energy (I)	5.1838 eV
Electron affinity (EA)	1.3954 eV
Electronegativity (χ)	3.2896 eV

Chemical hardness (η)	1.8942 eV
Chemical softness (S)	0.5279 eV-1
Chemical potential (μ)	-3.2896 eV
Global electrophilicity index (ω)	2.8565 eV
Maximum number of electrons transferred (ΔNmax)	1.7367 eV

Table 4: Absorption energies (λ in nm), oscillator strength (*f*), and transitions computed at TD-DFT B3LYP/6-311++G (d,p) level of theory and experimental UV-Visible wavelength (given in bracket and made bold)

Gas phase				DMSO			
Config	**Coefficient**	**f**	**λ, nm**	**Config**	**Coefficient**	**f**	**λ, nm**
103 ->104	0.69812	0.4625	372.49	103 ->104	0.69414	0.3611	371.88 **(382.07)**

Config – Configuration

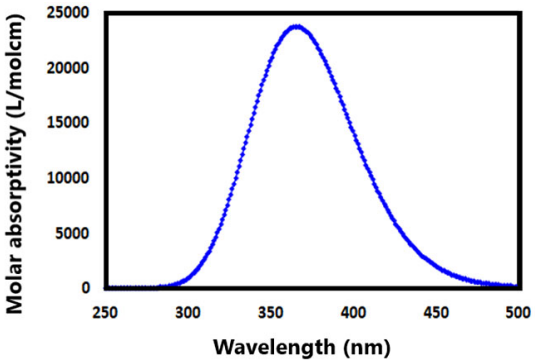

Fig. 6A: Theoretical UV-Visible spectrum in gas phase

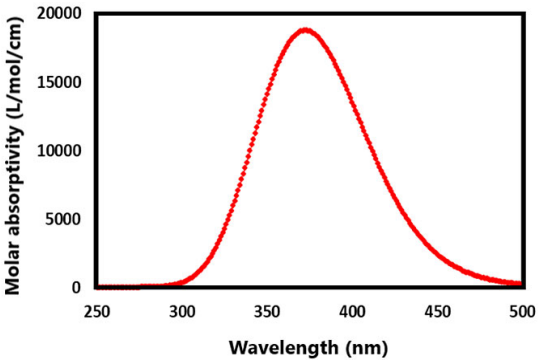

Fig. 6B: Theoretical UV-Visible spectrum in DMSO solvent

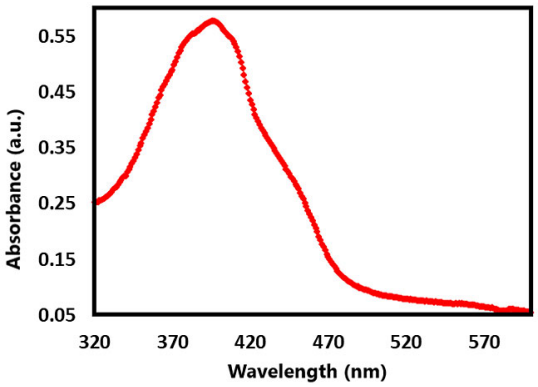

Fig. 6C: Experimental UV-Visible spectrum in DMSO solvent

The exploration suggests that the title compound has a low band energy gap and therefore will ease in the charge transfer phenomenon within the molecule. The maximum charge transfer is occurring in the molecule is 1.7367 eV. The global electrophilicity index is = 2.8565 eV. Absorption energies (λ in nm), excitation energy (eV), oscillator strength (*f*) and transitions have been established by computing the results at TD-B3LYP/6-311++G (d,p) level of theory for B3LYP/6-311++G (d,p) optimized geometries and this data is furnished in Table 4. The theoretical UV-Visible spectrum is given in Figure 6A (gas phase) and Figure 6B (DMSO). The experimental UV-Visible spectrum is recorded in the DMSO solvent and depicted in Figure 6C. From the computed UV-Visible analysis, it can be concluded here that the DMSO solvent has a blueshift effect on the absorption wavelength of the title compound. The bandgap in the DMSO solvent is higher than the gas phase UV-Visible spectrum. The theoretical absorption wavelength in the DMSO solvent is 371.88 nm and the experimental absorption wavelength in the DMSO solvent is 382.07 nm. There is good agreement between the theoretical UV-Visible spectrum (DMSO) and the experimental UV-Visible spectrum (DMSO).

Vibrational Assignments and Thermochemical Study

The theoretical and experimental IR spectra of CPMPP molecule are represented in Figure 7A and 7B respectively. The comparative investigations between the scaled theoretical and experimental IR frequencies are tabulated in Table 5. The total numbers of atoms in the titled molecule are 49 and therefore it will have 141 fundamental modes of vibrations. The point group symmetry is C1. The DFT computed IR spectrum overestimates the vibrational frequencies and therefore a scaling factor of 0.9613 has been used to correct the vibrational assignments. The results obtained in the theoretical results are showing good agreement with those obtained in experimental data.

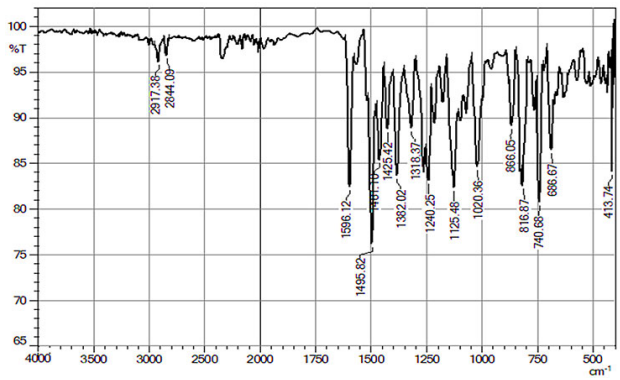

Fig. 7A: Experimental FT-IR spectrum

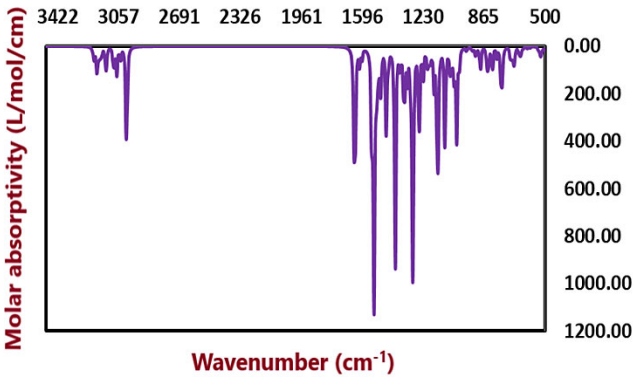

Fig. 7B: Experimental FT-IR spectrum

Table 5: Selected experimental and theoretical vibrational assignments of studied compound calculated at B3LYP/6-311++ G (d,p) level

Mode	Computed scaled frequencies (cm^{-1})	IR Intensity (km) mol^{-1}	Experimental frequencies (cm^{-1})	Assignment
75	1057	69.76	1020	Ar-Cl str
91	1242	244.74	1240	Ring C Ar-H ip bend
98	1307	12.75	-	Ring A Ar-H ip bend
100	1343	318.17	1318	C9-N7 str
101	1381	14.73	1382	C3-H6 ip bend
106	1430	10.22	1425	C41-H42, C41-H44 ip bend
113	1479	103.56	1495	Ring C aro C=C str
115	1549	17.72	-	Ring A aro C=C str
116	1551	2.50	-	Ring B aro C=C str
120	1583	41.79	1596	C=N str
122	2891	24.92	2844	C3-H6 str
130	3036	8.15	2917	C30-H33 str
131	3039	4.84	-	C14-H18, C16-H19, C12-H17 str
138	3081	4.70	-	Ring C Ar-H str

Abbreviations: Ar-aryl, str-stretching, ip bend- in plane bending, aro- aromatic, Ring A: phenyl ring, Ring B: 4-chlorophenyl ring, Ring C: 3,4-dimethoxyphenyl ring.

Table 6: Thermochemical parameters by DFT/B3LYP with 6-311++G (d,p) basis set

Parameters	Value
Total E Thermal kcal/mol	259.79
Translational	0.889
Rotational	0.889
Vibrational	258.01
Total Molar capacity at constant volume (Cv) Cal $mol^{-1}Kelvin^{-1}$	95.52
Translational	2.98
Rotational	2.98
Vibrational	89.56
Total entropy (S) Cal $mol^{-1}Kelvin^{-1}$	177.67
Translational	43.79
Rotational	36.99
Vibrational	96.897
Zero-point vibrational energy (kcal/mol)	244.14
Rotational Constant (GHz)	0.21726
	0.07687
	0.06175
E (RB3LYP) (a.u.)	-1609.51
Dipole moment (Debye)	4.59

Various thermodynamic functions have been obtained from the harmonic vibrational frequencies and are presented in the Table 6. The thermochemical parameters like Total energy (thermal), total molar heat capacity (Cv), total entropy (S), zero-point vibrational energy, and rotational constants have been established. Importantly, on the basis of the data provided in this, one can estimate other thermodynamic function with the help of their thermodynamic relationships.

Conclusion

In summary, pyrazoline derivative is synthesized from chalcones. For a detailed structural examination, spectroscopic, and quantum chemical analysis density functional theory (DFT) method with a basis set 6-311++G (d,p) has been employed. The geometry of the molecule was optimized by using a 6-311++G (d,p) basis set and the geometrical parameters like bond lengths and bond angles have been computed at the same level of theory. The frontier molecular orbital study has been effectively presented to analyze the chemical reactivity of the molecule. By using HOMO-LUMO energies various electron and quantum chemical parameters have been established. Absorption energies, oscillator strength, and electronic excitations have been calculated at TD-6-311++G (d,p) level of theory for 6-311++G (d,p) optimized geometries. The UV-Visible analysis suggests that there is good agreement between the theoretical UV-Visible spectrum (DMSO) and the experimental one. The C2 carbon atom is the most electronegative whereas C20 carbon atom is the most electropositive carbon atom. The scaled theoretical vibrational bands have been compared with the experimental frequencies and a good deal of agreement has found.

Acknowledgments

Authors acknowledge central instrumentation facility (CIF), Savitribai Phule Pune University, Pune for NMR, MGV's Pharmacy College, Nashik for UV-Visible, and central instrumentation centre (CIC), KTHM College, Nashik for FT-IR spectral analysis. Authors would like to express their sincere and humble gratitude to Prof. Arun B. Sawant for Gaussian study. Dr. Aapoorva P. Hiray, Coordinator, MG Vidyamandir institute, Nashik is gratefully acknowledged for Gaussian package.

Funding

We have not received any kind of fund for the research work.

Conflict of Interest

Authors declared that he do not have any conflict of interest regarding this research article.

References

1. Alam, M.J., Alam, O., Alam, P. and Naim, M.J., 2015. A review on pyrazole chemical entity and biological activity. *International Journal of Pharmaceutical Sciences and Research,* 6, pp.1433-1442.
2. Chauhan, A., Sharma, P.K. and Kaushik, N., 2011. Pyrazole: a versatile moiety. *International Journal of ChemTech Research,* 3(1), pp.11-17.
3. Karrouchi, K., Radi, S., Ramli, Y., Taoufik, J., Mabkhot, Y.N. and Al-Aizari, F.A., 2018. Synthesis and pharmacological activities of pyrazole derivatives: a review. Molecules, 23(1), p.134.
4. Balbi, A., Anzaldi, M., Macciò, C., Aiello, C., Mazzei, M., Gangemi, R., Castagnola, P., Miele, M., Rosano, C. and Viale, M., 2011. Synthesis and biological evaluation of novel pyrazole derivatives with anticancer activity. *European Journal of Medicinal Chemistry,* 46(11), pp.5293-5309.
5. Xu, Z., Gao, C., Ren, Q.C., Song, X.F., Feng, L.S. and Lv, Z.S., 2017. Recent advances of pyrazole-containing derivatives as anti-tubercular agents. *European Journal of Medicinal Chemistry,* 139, pp.429-440.
6. Rahimizadeh, M., Pordel, M., Bakavoli, M., Rezaeian, S. and Sadeghian, A., 2010. Synthesis and antibacterial activity of some new derivatives of pyrazole. *World Journal of Microbiology and Biotechnology,* 26(2), pp.317-321.
7. Hassan, S.Y., 2013. Synthesis, antibacterial and antifungal activity of some new pyrazoline and pyrazole derivatives. *Molecules,* 18(3), pp.2683-2711.

8. El-Moghazy, S.M., Barsoum, F.F., Abdel-Rahman, H.M. and Marzouk, A.A., 2012. Synthesis and anti-inflammatory activity of some pyrazole derivatives. *Medicinal Chemistry Research,* 21(8), pp.1722-1733.
9. Mironov, M.E., Poltanovich, A.I., Rybalova, T.V., Dolgikh, M.P., Tolstikova, T.G. and Shults, E.E., 2020. Synthesis and analgesic activity of 1, 3, 5-trisubstituted pyrazoles containing a diterpenoid moiety. *Russian Chemical Bulletin*, 69, pp.537-546.
10. Naim, M.J., Alam, O., Farah Nawaz, M., Alam, J. and Alam, P., 2016. Current status of pyrazole and its biological activities. *Journal of Pharmacy & Bioallied Sciences,* 8(1), p.2.
11. López-Viseras, M.E., Fernández, B., Hilfiker, S., González, C.S., González, J.L., Calahorro, A.J., Colacio, E. and Rodríguez-Diéguez, A., 2014. In vivo potential antidiabetic activity of a novel zinc coordination compound based on 3-carboxy-pyrazole. *Journal of inorganic biochemistry,* 131, pp.64-67.
12. Bekhit, A.A., Hymete, A., Asfaw, H. and Bekhit, A.E.D.A., 2012. Synthesis and Biological Evaluation of Some Pyrazole Derivatives as Anti-Malarial Agents. *Archiv der Pharmazie,* 345(2), pp.147-154.
13. Adole, V.A., Pawar, T.B., Koli, P.B. and Jagdale, B.S., 2019. Exploration of catalytic performance of nano-La2O3 as an efficient catalyst for dihydropyrimidinone/thione synthesis and gas sensing. *Journal of Nanostructure in Chemistry,* 9(1), pp.61-76.
14. Fahim, A.M. and Shalaby, M.A., 2019. Synthesis, biological evaluation, molecular docking and DFT calculations of novel benzenesulfonamide derivatives. *Journal of Molecular Structure,* 1176, pp.408-421.
15. de Marco, B.A., Rechelo, B.S., Tótoli, E.G., Kogawa, A.C. and Salgado, H.R.N., 2019. Evolution of green chemistry and its multidimensional impacts: A review. *Saudi pharmaceutical journal*, 27(1), pp.1-8.
16. Adole, V.A., Pawar, T.B. and Jagdale, B.S., 2020. Aqua-mediated rapid and benign synthesis of 1,2,6,7-tetrahydro-8H-indeno[5,4-b]furan-8-one-appended novel 2-arylidene indanones of pharmacological interest at ambient temperature. *Journal of the Chinese Chemical Society*, 67(2), pp.306-315.
17. Patil, B.N., Sathe, P.A., Parade, B.S., Vadagaonkar, K.S. and Chaskar, A.C., 2018. Transition metal free one pot synthesis of aryl carboxylic acids via dehomologative oxidation of styrenes. *Tetrahedron Letters,* 59(49), pp.4340-4343.
18. Adole, V.A., Jagdale, B.S., Pawar, T.B. and Sagane, A.A., 2020. Ultrasound promoted stereoselective synthesis of 2,3-dihydrobenzofuran appended chalcones at ambient temperature. *South African Journal of Chemistry*, 73, pp.35-43.
19. Patil, B.N., Lade, J.J., Karpe, A.S., Pownthurai, B., Vadagaonkar, K.S., Mohanasrinivasan, V. and Chaskar, A.C., 2019. Transition metal-catalyzed CH functionalization of arylacetic acids for the synthesis of benzothiadiazine 1, 1-dioxides. *Tetrahedron Letters,* 60(13), pp.891-894.
20. Adole, V.A., 2020. Synthetic approaches for the synthesis of dihydropyrimidinones/thiones (Biginelli adducts): a concise review. *World Journal of Pharmaceutical Research*, 9(6), pp. 1067-1091.
21. Adole, V.A., More, R.A., Jagdale, B.S., Pawar, T.B. and Chobe, S.S., 2020. Efficient Synthesis, Antibacterial, Antifungal, Antioxidant and Cytotoxicity Study of 2-(2-Hydrazin*eyl) thiazole Derivatives.* ChemistrySelect, 5(9), pp.2778-2786.
22. Patnala, H., Abbo, H.S., Potla, K.M., Titinchi, S.J. and Chinnam, S., 2019. Polyethylene glycol (PEG-400): An efficient one-pot green synthesis and anti-viral activity of novel α-diaminophosphonates. *Phosphorus, Sulfur, and Silicon and the Related Elements,* 194(11), pp.1035-1039.
23. Chobe, S.S., Adole, V.A., Deshmukh, K.P., Pawar, T.B. and Jagdale, B.S., 2014. Poly (ethylene glycol)(PEG-400): A green approach towards synthesis of novel pyrazolo [3, 4-d] pyrimidin-6-amines derivatives and their antimicrobial screening. *Archives of Applied Science Research,* 6(2), pp.61-66.
24. Subramanian, N., Sundaraganesan, N. and Jayabharathi, J., 2010. Molecular structure, spectroscopic (FT-IR, FT-Raman, NMR, UV) studies and first-order molecular hyperpolarizabilities of 1, 2-bis (3-methoxy-

4-hydroxybenzylidene) hydrazine by density functional method. *Spectrochimica Acta Part A: Molecular and Biomolecular Spectroscopy,* 76(2), pp.259-269.

25. Adole, V.A., Jagdale, B.S., Pawar, T.B. and Sawant, A.B., 2020. Experimental and theoretical exploration on single crystal, structural, and quantum chemical parameters of (E)-7-(arylidene)-1,2,6,7-tetrahydro-8H-indeno[5,4-b]furan-8-one derivatives: A comparative study. *Journal of the Chinese Chemical Society.*
26. Raja, M., Muhamed, R.R., Muthu, S. and Suresh, M., 2017. Synthesis, spectroscopic (FT-IR, FT-Raman, NMR, UV–Visible), NLO, NBO, HOMO-LUMO, Fukui function and molecular docking study of (E)-1-(5-bromo-2-hydroxybenzylidene) semicarbazide. *Journal of Molecular Structure,* 1141, pp.284-298.
27. Adole, V.A., Waghchaure, R.H., Jagdale, B.S., Pawar, T.B. and Pathade, S.S., Molecular tructure, frontier molecular orbital and spectroscopic examination on dihydropyrimidinones: *a comparative computational approach Journal of Advanced Scientific Research*, 2020. 11 (2), pp.64-70.
28. Raja, M., Muhamed, R.R., Muthu, S., Suresh, M. and Muthu, K., 2017. Synthesis, spectroscopic (FT-IR, FT-Raman, NMR, UV–Visible), Fukui function, antimicrobial and molecular docking study of (E)-1-(3-bromobenzylidene) semicarbazide by DFT method. *Journal of Molecular Structure,* 1130, pp.374-384.
29. Alaşalvar, C., Öztürk, N., Alaa, A.M., Gökce, H., El-Azab, A.S., El-Gendy, M.A. and Sert, Y., 2018. Molecular structure, Hirshfeld surface analysis, spectroscopic (FT-IR, Laser-Raman, UV–vis. and NMR), HOMO-LUMO and NBO investigations on N-(12-amino-9, 10-dihydro-9, 10-ethanoanthracen-11-yl)-4-methylbenzenesulfonamide. *Journal of Molecular Structure,* 1171, pp.696-705.
30. Adole, V.A., Waghchaure, R.H., Jagdale, B.S. and Pawar, T.B., 2020. Investigation of Structural and Spectroscopic Parameters of Ethyl 4-(4-isopropylphenyl)-6-methyl-2-oxo-1,2,3,4-tetrahydropyrimidine-5-carboxylate: a DFT Study. *Chemistry & Biology Interface*, 10(1).
31. Sarojinidevi, K., Subramani, P., Jeeva, M., Sundaraganesan, N., SusaiBoobalan, M. and VenkatesaPrabhu, G., 2019. Synthesis, molecular structure, quantum chemical analysis, spectroscopic and molecular docking studies of N-(Morpholinomethyl) succinimide using DFT method. *Journal of Molecular Structure,* 1175, pp.609-623.
32. Shakila, G., Saleem, H. and Sundaraganesan, N., 2017. FT-IR, FT-Raman, NMR and UV Spectral investigation: Computation of vibrational frequency, chemical shifts and electronic structure calculations of 1-bromo-4-nitrobenzene. *World Scientific News*, 61(2), pp.150-185.
33. Khamees, H.A., Mohammed, Y.H., Swamynayaka, A., Al-Ostoot, F.H., Sert, Y., Alghamdi, S., Khanum, S.A. and Madegowda, M., 2019. Molecular structure, DFT, vibrational spectra with fluorescence effect, hirshfeld surface, docking simulation and antioxidant activity of thiazole derivative. *ChemistrySelect,* 4(15), pp.4544-4558.
34. Pandey, M., Muthu, S. and Gowda, N.N., 2017. Quantum mechanical and spectroscopic (FT-IR, FT-Raman, 1H, 13C NMR, UV-Vis) studies, NBO, NLO, HOMO, LUMO and Fukui function analysis of 5-Methoxy-1H-benzo [d] imidazole-2 (3H)-thione by DFT studies. *Journal of Molecular Structure*, 1130, pp.511-521.
35. Selvaraj, S., Rajkumar, P., Kesavan, M., Thirunavukkarasu, K., Gunasekaran, S., Devi, N.S. and Kumaresan, S., 2020. Spectroscopic and structural investigations on modafinil by FT-IR, FT-Raman, NMR, UV–Vis and DFT methods. Spectrochimica Acta Part A: *Molecular and Biomolecular Spectroscopy,* 224, p.117449.
36. Moghanian, H., Mobinikhaledi, A. and Monjezi, R., 2013. Synthesis, spectroscopy (vibrational, NMR and UV–vis) studies, HOMO–LUMO and NBO analysis of 8-formyl-7-hydroxy-4-methylcoumarin by ab initio calculations. *Journal of Molecular Structure,* 1052, pp.135-145.
37. Sadgir NV, Dhonnar SL, Jagdale BS, Sawant AB. Synthesis, spectroscopic characterization, XRD crystal structure, DFT and antimicrobial study of (2E)-3-(2, 6-dichlorophenyl)-1-(4-

methoxyphenyl)-prop-2-en-1-one. *SN Applied Sciences*. 2020 Aug;2(8):1-2.

38. Chandralekha, B., Rajagopal, H., Muthu, S. and Sevvanthi, S., 2020. Spectroscopic (FT-IR, FT-RAMAN, NMR, UV–Vis) investigations, computational analysis and molecular docking study of 5-bromo-2-hydroxy pyrimidine. *Journal of Molecular Structure*, p.128494.
39. Murugavel, S., Ravikumar, C., Jaabil, G. and Alagusundaram, P., 2019. Synthesis, crystal structure analysis, spectral investigations (NMR, FT-IR, UV), DFT calculations, ADMET studies, molecular docking and anticancer activity of 2-(1-benzyl-5-methyl-1H-1,2,3-triazol-4-yl)-4-(2-chlorophenyl)-6-methoxypyridine–a novel potent human topoisomerase IIα inhibitor. J*ournal of Molecular Structure,* 1176, pp.729-742.
40. Jagdale, B.S. and Pathade, S.S., 2019. Synthesis, Characterization and Theoretical Study of 3-(4-bromophenyl)5-(2,4-dichlorophenyl)-1-phenyl-4,5-dihydro-1H-*pyrazole Journal of Applicable Chemistry*, 8(1), pp.12-19.
41. Hiremath, S.M., Khemalapure, S.S., Hiremath, C.S., Patil, A.S. and Basanagouda, M., 2020. Quantum chemical computational and spectroscopic (IR, Raman, NMR, and UV) studies on the 5-(5-methoxy-benzofuran-3-ylmethyl)-3H-[1,3,4] oxadiazole-2-thione. *Journal of Molecular Structure*, p.128041.
42. Manjusha, P., Muthu, S. and Raajaraman, B.R., 2020. Density functional studies and spectroscopic analysis (FT-IR, FT-Raman, UV–visible, and NMR) with molecular docking approach on an antifibrotic drug Pirfenidone. *Journal of Molecular Structure,* 1203, p.127394.
43. Tagore, S.S., Swaminathan, J., Manikandan, D., Gomathi, S., Ram, S.N., Ramalingam, M. and Sethuraman, V., 2020. Molecular, vibrational (FT-IR and FT-Raman), NMR and UV spectral analysis of imidazo [1, 2-b] pyridazine using experimental and DFT calculations. *Chemical Physics Letters,* 739, p.136943.
44. Khemalapure, S.S., Katti, V.S., Hiremath, C.S., Basanagouda, M., Hiremath, S.M., Armaković, S.J. and Armaković, S., 2019. Molecular structure, optoelectronic properties, spectroscopic (FT-IR, FT-Raman and UV–Vis), H-BDE, NBO and drug likeness investigations on 7, 8-benzocoumarin-4-acetic acid (7BAA). *Journal of Molecular Structure,* 1195, pp.815-826.
45. Aayisha, S., Devi, T.R., Janani, S., Muthu, S., Raja, M. and Sevvanthi, S., 2019. DFT, molecular docking and experimental FT-IR, FT-Raman, NMR inquisitions on "4-chloro-N-(4, 5-dihydro-1H-imidazol-2-yl)-6-methoxy-2-methylpyrimidin-5-amine": Alpha-2-imidazoline receptor agonist antihypertensive agent. *Journal of Molecular Structure*, 1186, pp.468-481.
46. Frisch MJ, Trucks GW, Schlegel HB, Scuseria GE, Robb MA, Cheeseman JR, Montgomery Jr JA, Vreven T, Kudin KN, Burant JC, Millam JM. Gaussian 03 (Revision E. 01), Gaussian, Inc, Wallingford CT, 2004